NASA/TM—2010-216816 JANNAF 1211

NASA's Evolutionary Xenon Thruster (NEXT) Project Qualification Propellant Throughput Milestone: Performance, Erosion, and Thruster Service Life Prediction After 450 kg

Daniel A. Herman
Glenn Research Center, Cleveland, Ohio

November 2010

NASA STI Program . . . in Profile

NASA/TM—2010-216816 JANNAF 1211

NASA's Evolutionary Xenon Thruster (NEXT) Project Qualification Propellant Throughput Milestone: Performance, Erosion, and Thruster Service Life Prediction After 450 kg

Daniel A. Herman
Glenn Research Center, Cleveland, Ohio

Prepared for the
57th Joint Army-Navy-NASA-Air Force (JANNAF) Propulsion Meeting
sponsored by the JANNAF Interagency Propulsion Committee
Colorado Springs, Colorado, May 3–7, 2010

National Aeronautics and
Space Administration

Glenn Research Center
Cleveland, Ohio 44135

November 2010

This report contains preliminary findings,
subject to revision as analysis proceeds.

Level of Review: This material has been technically reviewed by technical management.

Available from

NASA Center for Aerospace Information
7115 Standard Drive
Hanover, MD 21076–1320

National Technical Information Service
5301 Shawnee Road
Alexandria, VA 22312

Available electronically at http://gltrs.grc.nasa.gov

NASA's Evolutionary Xenon Thruster (NEXT) Project Qualification Propellant Throughput Milestone: Performance, Erosion, and Thruster Service Life Prediction After 450 kg

Daniel A. Herman
National Aeronautics and Space Administration
Glenn Research Center
Cleveland, Ohio 44135

Abstract

The NASA's Evolutionary Xenon Thruster (NEXT) program was awarded the task of developing an ion propulsion system that significantly improves and extends the current state-of-the-art capabilities. One area that NEXT surpasses the current state-of-the-art NASA Solar Electric Propulsion Technology Applications Readiness (NSTAR) ion propulsion system is the thruster service life capability. The service life capability of the NEXT ion thruster is being assessed by a comprehensive validation scheme utilizing a combination of testing and analysis. An ongoing NEXT Long-Duration Test (LDT) provides conclusive quantification of accelerator grid erosion, the predicted first failure mode, while operating for thousands of hours at various conditions spanning the broad NEXT throttling range. The thruster has set records for the most propellant processed and highest total impulse demonstrated for any high-technology readiness level electric propulsion thruster. The NEXT project qualification throughput requirement was set at 450 kg based upon individual thruster throughput requirements from multiple mission analyses (maximum of 300 kg) with 50 percent margin. The NEXT LDT surpassed this milestone in December 2009.

Thruster performance characteristics, measured over the entire throttle range of the thruster, have been within pretest predictions showing little signs of degradation. Erosion of critical thruster components have been monitored via in-situ cameras illustrating mitigation of two of the critical NSTAR wear-out mechanisms: accelerator aperture barrel erosion leading to failure to prevent electron backstreaming (the NSTAR first failure mode) and discharge cathode assembly erosion. The predicted first failure mode for the NEXT thruster is erosion of the accelerator grid by charge-exchange ions leading to the eventual loss of the structural integrity of the accelerator grid. Pretest modeling of the accelerator groove penetration depth as a function of time for the entire throttle table has been validated at five operating conditions (spanning the throttle range) for which extended thruster operations have been performed.

Groove erosion model predictions and data are in agreement predicting penetration at the highest groove erosion rate at full input power, providing a minimum thruster service life, after 750 kg throughput. Following the planned mission-like throttling profile, the thruster will transition back to full-power until failure. With this aggressive throttling strategy, 64 percent of total time at full-power, the NEXT first failure is expected to be reached after 45 kh of operation processing over 800 kg of xenon.

Nomenclature

BOL	beginning-of-life
DCA	discharge cathode assembly
DCIU	digital control interface unit
DS1	Deep Space 1 mission
DSDRM	deep space design reference mission
ELT	extended life test
EM	engineering model
EM3	engineering model 3 thruster
GRC	NASA Glenn Research Center

IPS	ion propulsion system
I_{sp}	specific impulse, s
J_B	beam current, A
J_{NK}	neutralizer keeper current, A
LDT	long-duration test
m_C	discharge cathode flow rate, sccm
m_M	main plenum flow rate, sccm
m_N	neutralizer cathode flow rate, sccm
NCA	neutralizer cathode assembly
NEAR	Near Earth Asteroid Rendezvous mission
NEXT	NASA's Evolutionary Xenon Thruster
NSTAR	NASA Solar Electric Propulsion Technology Application Readiness
P_{IN}	thruster input power, kW
PM	prototype model
SSR	surface sample return
T	thrust, mN
TL	throttle level
TT10	throttle table 10
V_A	accelerator grid voltage, V
V_B	beam power supply voltage, V
φ	aperture or orifice diameter

Introduction

The success of the NASA Solar Electric Propulsion Technology Applications Readiness (NSTAR) ion propulsion system on Deep Space 1 (DS1) secured the future for ion propulsion technology for future NASA missions (Ref. 1 and 2). Three NSTAR thrusters are currently propelling the Dawn spacecraft on its mission to the two heaviest main-belt asteroids, Ceres and Vesta (Ref. 3). Analyses conducted at NASA identified the need for a higher-power, higher-thrust, and higher total throughput capability ion propulsion system beyond the 2.3 kW NSTAR ion thruster targeted for robotic exploration of the outer planets.

The NASA Glenn Research Center (GRC)-led team has developed the next generation ion propulsion system called NASA's Evolutionary Xenon Thruster (NEXT). The NEXT ion propulsion system (IPS) has demonstrated significant enhancements beyond current state-of-the-art systems to provide future NASA science missions with enhanced mission capabilities at a low total development cost. Phase 2 of the program develops flight-like engineering model components, with sufficient performance, functional, environmental, integration, and lifetime testing, to validate the technology approach and hardware design. The NEXT project has developed flight-like engineering model components that have all passed environmental testing at qualification levels, with the exception of the power-processing unit (which is ongoing). A system integration test with the highest-fidelity hardware has recently been executed demonstrating that the NEXT IPS is at a technology readiness level of 6 (when power processor environmental is completed) and is ready for mission opportunities. An update of the NEXT program can be found in Reference 4. The NEXT IPS is applicable to a wide range of NASA solar system exploration missions, as well as earth-space commercial and other missions of national interest. NEXT affords larger delivered payloads, smaller launch vehicle size, and other mission enhancements compared to chemical and other electric propulsion technologies for Discovery, New Frontiers, Mars Exploration, and Flagship outer-planet exploration missions (Refs. 5 to 7).

The NEXT system consists of a high-performance, 7 kW ion thruster[1]; a high-efficiency, modular, 7 kW power processing unit[2] with an efficiency and a specific power greater than NSTAR; a highly-

[1] Ion thruster development led by GRC; prototype-model fabrication by Aerojet (Redmond, Washington).

flexible, advanced xenon propellant management system[3] that utilizes proportional valves and thermal throttles to reduce mass and volume; a lightweight engine gimbal[4]; and key elements of a digital control interface unit (DCIU) including software algorithms (Refs. 8 to 14). The NEXT thruster and component technologies demonstrate a significant advancement in technology beyond the current state-of-the-art NSTAR thruster systems.

The NEXT thruster service life capability is being assessed via a comprehensive service life validation scheme utilizing a combination of test and analysis. The approach is consistent with the lifetime qualification standard for electric thrusters (Ref. 15). The NEXT ion thruster is an evolution of the NSTAR thruster design. All of the plasma physic processes that take place in the NEXT thruster occur in the NSTAR design. The NEXT thruster, as a second generation deep-space ion thruster, made use of over 58,000 h of ground and flight test experience (not including that from the ongoing Dawn mission) in both the design of the NEXT thruster and evaluation of thruster wear-out failure modes. A NEXT service life assessment was conducted at GRC employing several models to evaluate all known failure modes with high confidence based upon the substantial amount of ion thruster testing dating back to the early 1960s (Refs. 16 and 17). The NEXT service life assessment also incorporated the results of the NEXT 2,000 h wear test conducted on a NEXT engineering model ion thruster at 6.9 kW input power (Refs. 16 and 18). The transparency between engineering and prototype-model thruster wear characteristics has also been demonstrated by a short-duration prototype-model wear test (Refs. 19 and 20).

The NEXT IPS is designed for broad mission capture, thereby improving the return of investment, accomplished by a wide throttle range of varying specific impulse and thrust values. With widespread mission applicability, the project-level qualification throughput (i.e., thruster service life) was determined based upon the individual thruster requirements for proposed missions that would utilize the NEXT IPS. Nine mission analyses performed baselining the NEXT IPS for primary propulsion indicated a maximum individual thruster throughput requirement of 300 kg (Ref. 16). A margin of 50 percent was placed on this throughput requirement to form the project qualification throughput of 450 kg for the NEXT thruster. This 50 percent margin is based on an early Comsat requirement that thrusters be qualified for life by test with durations equal to 1.5 times the mission life (Ref. 15).

To validate the NEXT thruster service life model and qualify the NEXT thruster, a Long-Duration Test (LDT) was initiated. During the NEXT LDT, the thruster has been operated for extended duration at five operating conditions that span the throttle range in a mission-like profile that decreases the input power with testing duration, listed in Table 1. The five conditions were selected to capture the most severe erosion mechanisms, envelope the throttle table, and validate thruster service life model predictions. The original goal of the NEXT LDT was to demonstrate the project qualification propellant throughput requirement of 450 kg, while assessing thruster performance and erosion rates over the entire throttle range. Detailed thruster characterizations are periodically performed over 11 operating conditions covering the NEXT throttle table. The NEXT thruster service life analysis is being applied to assess thruster wear and performance for the specific throttling profiles of potential mission opportunities (Refs. 17 and 21). The life assessment predicts the earliest thruster failure, minimum thruster service life, occurring for full-power operation after greater than 750 kg of xenon throughput. All wear testing data support a NEXT thruster service life capability greater than 750 kg, well beyond the mission-derived propellant throughput requirement of 300 kg (Refs. 16 to 18, and 22 to 25).

---

[2] Power processing unit development led by L3 Comm ETI (Torrance, California).
[3] Propellant management system and DCIU simulator development led by Aerojet (Redmond, Washington).
[4] Gimbal development led by the NASA Jet Propulsion Laboratory and ATK (formerly Swales Aerospace).

TABLE 1.—NEXT LONG-DURATION TEST MISSION-LIKE THROTTLING STRATEGY

Input power, kW	Operating condition	Duration, kh	Segment throughput, kg	Segment total impulse, N·sec	End of segment date (or estimate)
6.9	3.52 A, 1800 V	13.0	267.4	1.09×10^{7}	November 17, 2007
4.7	3.52 A, 1179 V	6.5	129.8	4.44×10^{6}	December 23, 2008
1.1	1.20 A, 679 V	3.4	26.8	6.32×10^{5}	June 24, 2009
0.5	1.00 A, 275 V	3.2	23.4	3.33×10^{5}	December 15, 2009
2.4	1.20 A, 1800 V	3.0	22.8	8.66×10^{5}	(May 3, 2010)
	Totals	29.1	470.2	1.72×10^{5}	

NEXT Long-Duration Test Background

The NEXT LDT is being conducted in VF16 at GRC with an engineering model ion thruster, designated EM3, shown in Figure 1. The EM3 thruster has been modified to a flight-representative configuration by incorporating PM ion optics, delivered by industry partner Aerojet Corporation, and a graphite discharge cathode keeper electrode (Ref. 13). The NEXT thruster is nominally a 0.5 to 6.9 kW input power xenon ion thruster utilizing two-grid, dished-out ion optics. The technical approach for the NEXT design is a continuation of the derating philosophy used for the NSTAR ion thruster. A beam extraction area 1.6 times that of NSTAR allows higher thruster input power while maintaining low voltages and ion current densities, thus maintaining thruster longevity. Descriptions of the NEXT EM3 thruster design and VF16 can be found in References 19, 23, 24, and 26 to 29.

One of the unexpected findings from the NSTAR ELT was the anomalous discharge cathode keeper erosion, which was more severe and qualitatively different than prior 1,000 and 8,200 h NSTAR wear tests (Refs. 30 to 32). Due to the complete NSTAR ELT discharge cathode keeper faceplate erosion and the NEXT EM 2,000 h wear test results, a graphite discharge cathode keeper is employed on EM3, similar to the NEXT PM thruster design, to mitigate keeper erosion. The erosion rate of carbon due to the low-energy discharge plasma ion impacts is less than 1/20 that of molybdenum (Ref. 33), dramatically extending keeper service life. The predicted service life of the graphite keeper is in excess of 87 kh for the worst case operating condition (Ref. 16).

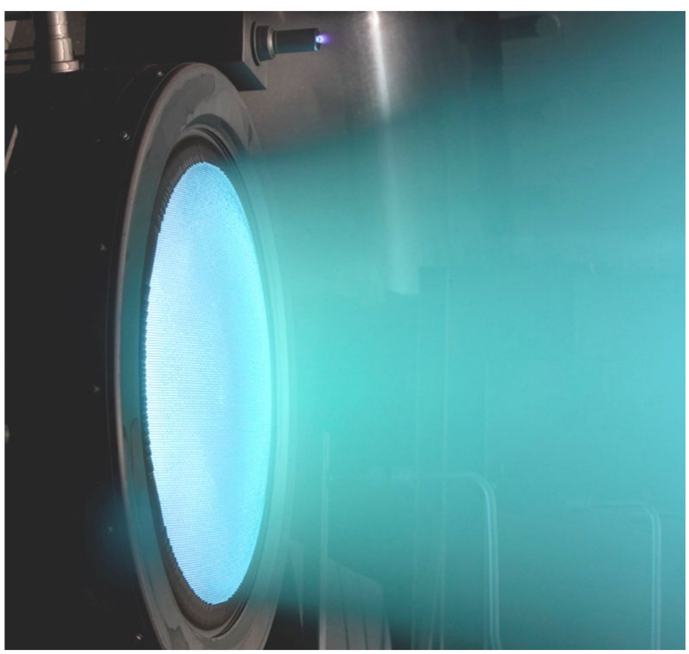

Figure 1.—NEXT EM3 operating at full power during the LDT.

Erosion of critical ion engine components is monitored by six in-situ, charge-coupled device cameras that capture erosion patterns and wear rates. The cameras record: the downstream neutralizer keeper and cathode orifice plate, the discharge cathode keeper and cathode orifice plate, accelerator grid apertures at various radial locations from centerline, and the cold grid-gap of the thruster ion optics. The cameras are mounted to a single-axis positioning system that moves the cameras radially in front of the thruster, typically while the thruster is not operating. Additional testing diagnostics include: a data acquisition system that monitors thruster telemetry at 15 Hz permitting autonomous operation, staggered planar probes to monitor beam profiles and divergence, a quartz-crystal microbalance to monitor backsputtered efflux, and a far-field ExB probe to measure the charge-state signature of the plume. Descriptions of the testing and facility diagnostics can be found in Refs. 22 and 23.

Results and Discussion

As of April 5, 2010, the NEXT EM3 thruster has accumulated 28,500 h of operation. The NEXT thruster has processed 466 kg of xenon; *nearly double the 235 kg total propellant throughput processed by the DS1 flight spare in the NSTAR Extended Life Test (ELT)*. Figure 2 shows the NEXT LDT propellant throughput as a function of elapsed time with reference to the NSTAR ELT and flight DS1 thruster, the thruster throughput requirements from various mission analyses conducted using the NEXT propulsion system, and the NEXT qualification level throughput of 450 kg (Refs. 34 to 36). The NEXT LDT demonstrated the project-level thruster throughput requirement of 450 kg in December 2009, achieving the primary goal of the LDT. The goal of the LDT was then redefined to demonstrate the thruster service life capability by operating the thruster to failure (resource restraints withstanding). The NEXT thruster has demonstrated a total impulse of 17 MN·s to date; *which is the highest total impulse ever demonstrated by an ion thruster.* The NEXT milestone is also the highest total impulse ever demonstrated by any sub-100 kW electric propulsion device (Ref. 37). The NEXT LDT demonstrated total impulse exceeded that of the 30,352 h NSTAR ELT in less than 1/3rd the thruster operating duration, shown in Figure 3.

The following section discusses the NEXT LDT results to date with emphasis on demonstrated thruster life metrics, thruster performance, and critical component erosion characteristics. Performance degradation will be compared to the pretest predictions and the NSTAR ELT. Observations and measurements of the erosion of critical components will be compared to the NSTAR ELT and the thruster service life assessment predictions.

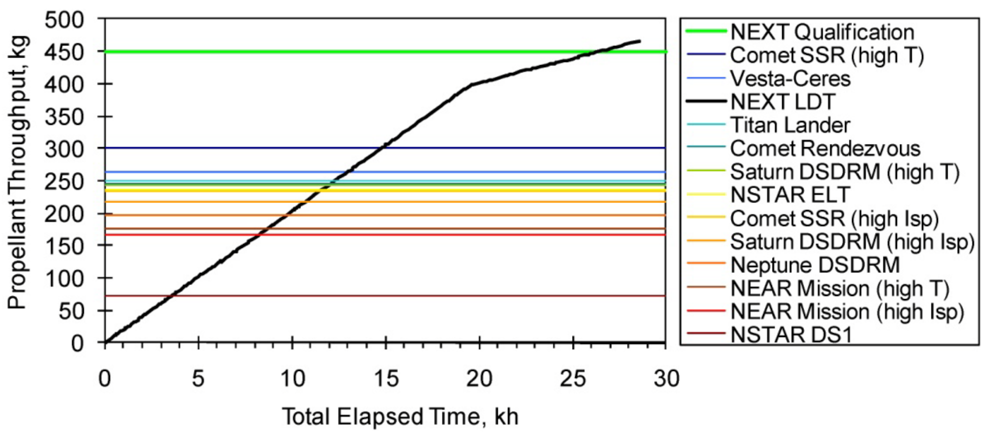

Figure 2.—NEXT LDT propellant throughput as a function of time with reference milestones. NEXT project qualification throughput (450 kg) was demonstrated in December 2009.

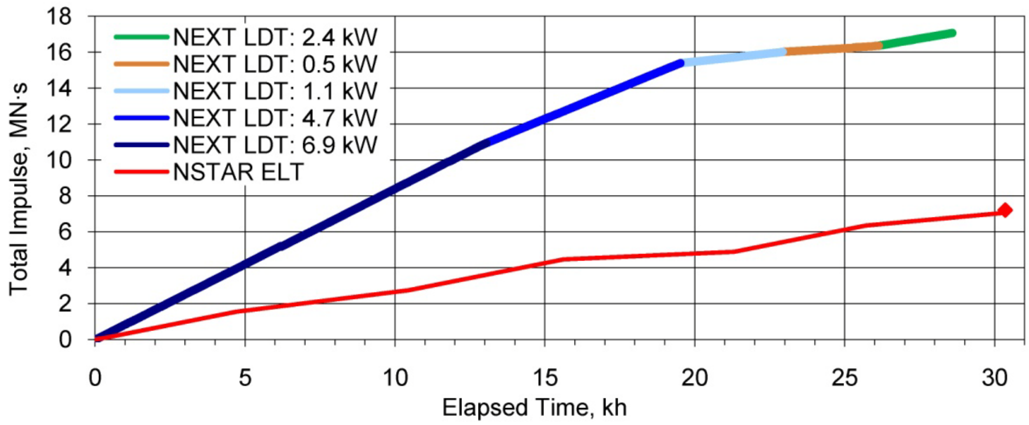

Figure 3.—NEXT LDT and NSTAR ELT total impulse data as a function of time.

NEXT Thruster Performance Data

Performance of the EM3 thruster has been steady with minimal degradation. Thruster performance measurement, calculation methodology, and assumptions are described in detail in Refs. 19, 27, 38, and 39. A summary of key thruster performance parameters comparing beginning-of-life (BOL) performance to performance after processing 300 kg (lifetime requirement) and 450 kg (qualification—150 percent lifetime requirement) of xenon is shown in Table 2. The table identifies the thruster operating condition by the unique combination of beam current and beam power supply voltage. Performance parameters are listed with the relevant associated uncertainties including: thruster input power, specific impulse, thrust efficiency, and discharge propellant utilization efficiency. Note that the pretest characterization testing was performed with a higher neutralizer flow rate for many operating conditions. An intentional decrease in neutralizer flow following the BOL characterization was made to improve overall propellant utilization efficiency resulting in increases in specific impulse and thrust efficiency. However, for medium and low-power conditions, the BOL neutralizer flow rate was not sufficient to prevent plume-mode operation of the neutralizer throughout the LDT. The loss of neutralizer flow margin with propellant processed has been addressed by a design change in the dimensions of the PM neutralizer and the release of an updated throttle table that increases the neutralizer flow rate setpoint as a function of propellant processed (Ref. 40). The neutralizer flow rate is shown in Table 2 to highlight the different values for the operating conditions at the various throughput milestones. All other input operating parameters for a given beam current and beam power supply voltage are identified in Table 3 and Table 4 of the Appendix.

The summary of thruster performance shows negligible performance degradation after 450 kg of xenon processed. Calculated thrust has remained constant while thruster input power, shown in Figure 4, has increased by as much as 30 W due to increasing discharge losses. Discharge losses increase due to, among other factors: accelerator grid aperture erosion that decreases the residence time of neutrals in the discharge chamber, increased thermal conductance from the discharge cathode emitter due to barium migration, and changes in surface conditions of the cathode emitter and anode collector (Ref. 20). Increases in thruster input power with thruster operating duration are the main areas of degradation anticipated for the IPS on a spacecraft. Beam voltage and beam current are fixed for a given operating condition; therefore variations in thrust can only be due to variations in beam divergence, variations in neutralizer coupling voltage, variations in double-ion content of the beam, or operation with electron backstreaming. Beam profiles obtained up to 13 kh have demonstrated a negligible change in the thruster plume divergence for any operating condition (Ref. 23). Coupling voltage and electron backstreaming margin have demonstrated little variability, which will be discussed later. A slight increase of a few percentage points in the double-ion signature of the beam has been measured by the far-field ExB probe due to increases in operating discharge voltage (Refs. 23 and 24).

TABLE 2.—NEXT LDT PERFORMANCE COMPARISON OF BOL (WHITE), AFTER 300 kg (SHADED 30 PERCENT), AND AFTER 450 kg (SHADED 50 PERCENT) XENON PROCESSED FOR CONDITIONS SPANNING THE NEXT THROTTLE TABLE

J_B, A	V_B, V	P_{IN}, kW	Calc. thrust, mN	Thrust uncertainty, mN	Isp, s	Isp uncertainty, s	Thrust efficiency	Thrust efficiency uncertainty	[a]Disch. prop. efficiency	m_N, sccm
3.52	**1800**	**6.83**	**237**	**± 3**	**4090**	**± 70**	**0.695**	**± 0.017**	**0.89**	**5.16**
3.52	**1800**	**6.86**	**237**	**± 3**	**4170**	**± 70**	**0.706**	**± 0.017**	**0.89**	**4.01**
3.52	**1800**	6.86	**237**	**± 3**	4170	**± 70**	0.706	**± 0.017**	0.89	4.01
3.52	1180	4.67	192	± 2	3320	± 60	0.666	± 0.017	0.89	5.16
3.52	1180	4.70	192	± 2	3380	± 60	0.676	± 0.017	0.89	4.01
3.52	1180	4.70	192	± 2	3380	± 60	0.676	± 0.017	0.89	4.01
2.70	1800	5.27	182	± 2	4020	± 70	0.680	± 0.017	0.89	4.75
2.70	1800	5.28	182	± 2	4130	± 70	0.696	± 0.017	0.89	3.50
2.70	1800	5.28	182	± 2	4100	± 70	0.692	± 0.017	0.89	3.82
2.70	1180	3.61	147	± 2	3260	± 60	0.652	± 0.017	0.890	4.75
2.70	1180	3.63	147	± 2	3350	± 60	0.666	± 0.017	0.89	3.50
2.70	1180	3.62	147	± 2	3330	± 60	0.662	± 0.017	0.89	3.82
2.00	1800	3.96	134	± 2	4060	± 70	0.673	± 0.017	0.93	4.41
2.00	1800	3.96	134	± 2	4230	± 70	0.701	± 0.017	0.93	3.00
2.00	1800	3.95	134	± 2	4130	± 70	0.686	± 0.017	0.93	3.78
2.00	1180	2.72	108	± 1	3290	± 60	0.642	± 0.017	0.93	4.41
2.00	1180	2.73	108	± 1	3420	± 60	0.666	± 0.017	0.93	3.00
2.00	1180	2.73	108	± 1	3340	± 60	0.651	± 0.017	0.93	3.78
1.20	1800	2.43	80	± 1.0	3800	± 70	0.615	± 0.017	0.93	4.01
1.20	1800	2.42	80	± 1.0	3890	± 70	0.632	± 0.017	0.93	3.50
1.20	1800	2.43	80	± 1.0	3750	± 70	0.609	± 0.017	0.93	4.28
1.20	1180	1.70	65	± 0.8	3090	± 50	0.581	± 0.017	0.93	4.01
1.20	1180	1.69	65	± 0.8	3180	± 50	0.602	± 0.017	0.93	3.30
1.20	1180	1.68	65	± 0.8	3040	± 50	0.576	± 0.017	0.93	4.28
1.20	679	1.12	49	± 0.6	2340	± 40	0.504	± 0.017	0.93	4.01
1.20	679	1.10	49	± 0.6	2380	± 40	0.521	± 0.017	0.93	3.50
1.20	679	1.10	49	± 0.6	2300	± 40	0.503	± 0.017	0.93	4.28
1.20	300	0.648	32	± 0.4	1510	± 30	0.365	± 0.017	0.93	4.01
1.20	300	0.651	32	± 0.4	1540	± 30	0.371	± 0.017	0.93	3.50
1.20	300	0.654	32	± 0.4	1500	± 30	0.359	± 0.017	0.93	4.28
1.00	275	0.518	26	± 0.3	1400	± 20	0.340	± 0.017	0.87	3.01
1.00	275	0.520	26	± 0.3	1360	± 20	0.329	± 0.017	0.87	3.50
1.00	275	0.523	26	± 0.3	1320	± 20	0.318	± 0.017	0.87	4.28

[a]Corrected for ingested mass flow

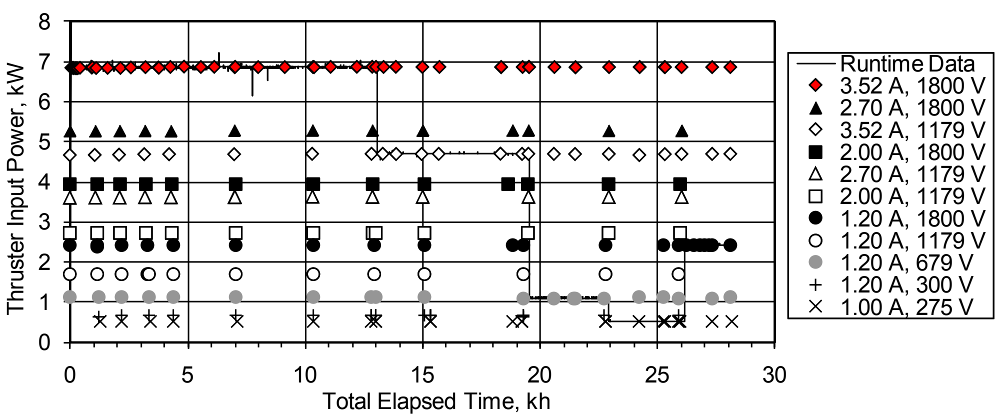

Figure 4.—NEXT LDT thruster input power data as a function of time.

Discharge propellant utilization efficiency has been nearly constant with variations of less than 0.5 percentage points, within the uncertainty of measured mass flow into the thruster, due to changes in ingested mass flow as the neutralizer flow rate is changed. Specific impulse and thrust efficiency values vary with the changes in neutralizer flow rate as expected and are shown in Figure 5 and Figure 6, respectively. There were improvements in both parameters for most operating conditions after 300 kg of xenon processed due to the decreased neutralizer flow rate following the pretest characterization. For conditions of medium and low beam current, the neutralizer flow rate has increased as a function of propellant throughput processed to maintain spot-mode operation (i.e., lower erosion, as described previously (Ref. 40)). The increasing neutralizer flow rate results in decreases in the specific impulse and thrust efficiency values. The maximum variations are 2.5 percentage point changes in thrust efficiency and 170 s in specific impulse. These modest decreases in thruster performance due to a need to increase neutralizer flow rate are well understood and expected. The increase in neutralizer flow rate requiring additional propellant, along with the associated decreases in thrust efficiency and specific impulse, are anticipated to have modest impacts on the spacecraft and mission trajectories.

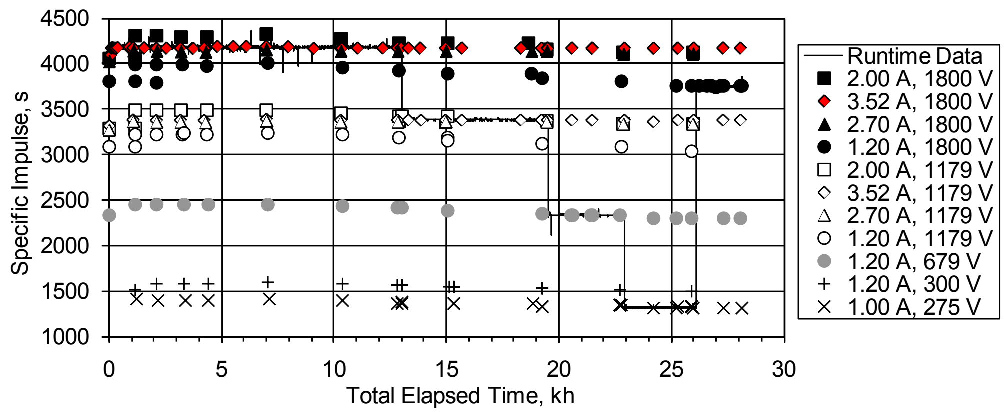

Figure 5.—NEXT LDT specific impulse data as a function of time.

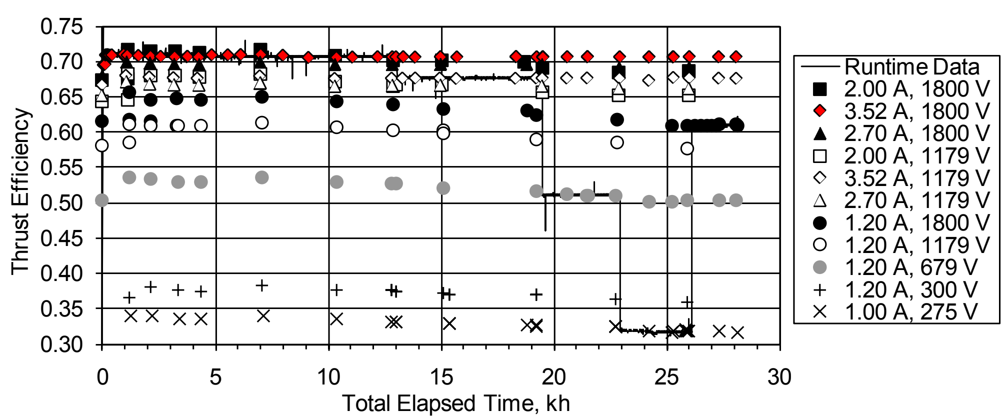

Figure 6.—NEXT LDT thrust efficiency data as a function of time.

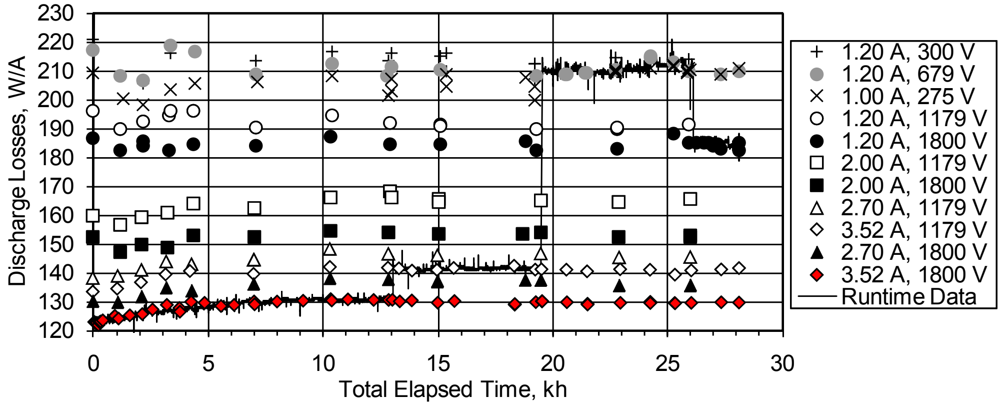

Figure 7.—NEXT LDT thruster discharge loss data as a function of time.

Discharge Chamber, Discharge Cathode, and Neutralizer Cathode

Performance values of the discharge cathode and discharge chamber during the life test are consistent with pretest predictions. Thruster discharge losses with time, which are the primary cause for increasing thruster input power, are plotted in Figure 7. The pretest prediction for the anticipated increase in discharge loss at full-power was 9 W/A. Full-power discharge loss data from the LDT increased from 122 to a maximum of 131 W/A over 450 kg throughput. Discharge losses stabilized after several thousands of hours of operation, consistent with observed trends in accelerator aperture erosion and discharge cathode voltage and current data. The former impacts the discharge losses by increasing neutralizer transmittance, requiring an increase in discharge emission current to maintain a fixed beam current. The latter may be due to changes in the cathode itself: changes in emitter surface conditions, increased thermal conductance from the emitter due to barium migration, or changes in the anode surface conditions due to thin film deposits to name a few (Ref. 20). Modest increases in discharge losses, less than 6 percent of pretest values, are observed for all operating conditions. Higher discharge loss variability is observed for lower power operating conditions that operate at higher discharge propellant utilization efficiencies where discharge loss variation is more sensitive to subtle flow variations.

The gradual 6 percent increase in discharge losses observed during the NEXT LDT translates into a predictable and less variable thruster performance compared to that of the NSTAR thruster. NSTAR thruster full-power discharge losses, considerably higher (~50 W/A) than NEXT due primarily to the smaller discharge chamber, increased by 10 to 15 W/A within the first 500 h of operation in three separate wear tests (Refs. 30, 31, and 41). The reduced BOL increase in discharge losses in the NEXT design is a result of a flatter NEXT beam profile, thicker accelerator grid, smaller-cusp/lower-variation ion optics, and more focused beamlets at the full-power operating condition. After processing 466 kg of propellant, the NEXT LDT full-power discharge losses increased by 9 W/A compared to the NSTAR ELT increase of 22 W/A after 210 kg (Refs. 32 and 42).

Discharge voltages have increased by approximately 1 V over the test duration of 28,500 h, shown in Figure 8. Discharge currents have increased slightly (≤0.5 A) after processing 466 kg (Ref. 22). Increased peak-to-peak variability in the discharge voltage is observed at low-power operating conditions due to sensitivity of the discharge cathode operation at higher discharge propellant utilization efficiencies and the result of an intermittent discharge keeper-to-common short that appeared after 13,875 h of operation (833 h after throttling to 4.7 kW). Discharge keeper voltage data are shown in

Figure 9. The electrical shorting of the discharge keeper to common was an expected event based upon the findings from the NEXT 2,000 h and the High Power Electric Propulsion 2,000 h wear tests (Refs. 18 and 43). Post-test analyses measured tungsten (with traces of barium) material deposits on the upstream surface of the keeper faceplate near the orifice of 40 and 70 µm thicknesses for the NEXT and High Power Electric

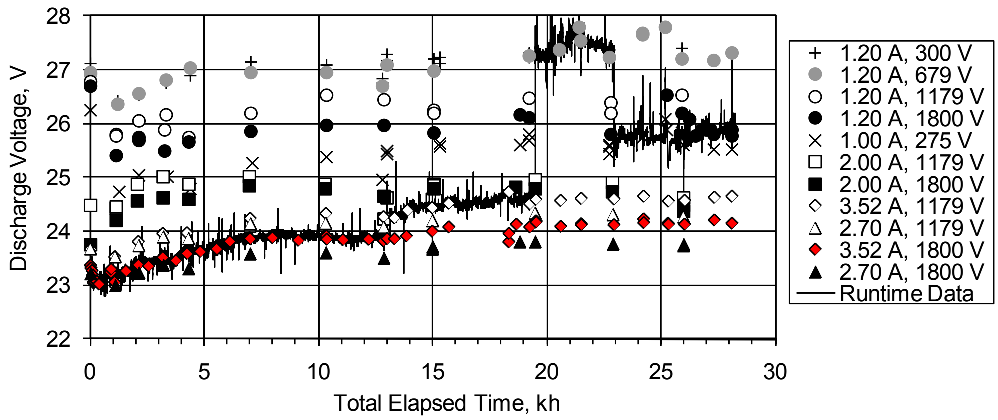

Figure 8.—NEXT LDT thruster discharge voltage data as a function of time.

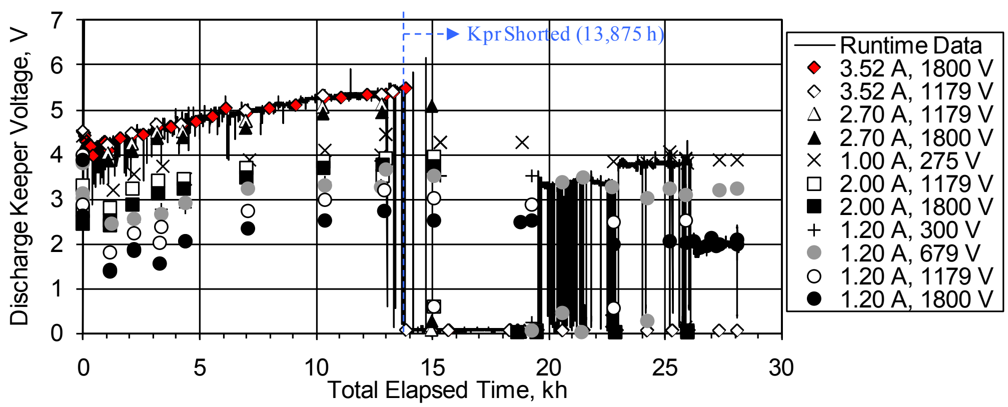

Figure 9.—NEXT LDT thruster discharge keeper voltage data as a function of time.

Propulsion wear tests, respectively (Refs. 44 and 45). Assuming linear growth, extrapolation of these thicknesses for extended duration would have resulted in bridging the estimated operating gap between the NEXT LDT keeper and cathode face after an operating duration on the order of 10 to 20 kh. The short appeared in the NEXT LDT after 13.9 kh, within the bounds of the two deposition rates. It should be mentioned that the NEXT lifetime assessment also predicted a priori this shorting event and considered its impact on thruster service life (Refs. 16 and 17).

The presence of the keeper electrical short does negatively impact discharge cathode ignition durations. For normal ignitions, that is with the keeper not shorted, the keeper electrode is at anode potential. The short distance between cathode and keeper (at anode potential), over which the discharge voltage and igniter pulses are applied, makes it easier for the cathode to ignite. With the keeper shorted to cathode, the discharge supply voltage is applied between the cathode and the anode that is much further away. Additionally, the current trickling through the keeper, and 1 kΩ resistor between the keeper and anode, can attenuate the igniter pulse. There have been 230 discharge cathode ignitions to date. Typically, ignition occurs within 5 min of application of the heater current. Longer ignitions have been observed (up to 32.5 min) due to the effects of facility regenerations, an increasing impedance for the heater current return path (that was eliminated in the PM cathode design), and effects of the keeper short (Ref. 22).

The neutralizer hollow cathode provides electrons to neutralize the space charge of the ion beam in order to prevent spacecraft charging. The neutralizer cathode utilizes a keeper electrode to ignite the cathode and to prevent the extinguishing of the neutralizer during thruster recycle events (i.e., when the high-voltage beam is cycled off and on). The NEXT EM3 ion thruster utilizes a neutralizer design that is mechanically similar to the hollow cathode assembly of the International Space Station plasma contactor (Ref. 46). Because the neutralizer cathode emission current range on the NEXT ion thruster is similar to that of the plasma contactor hollow cathode assembly, the NEXT neutralizer design can leverage the large cathode database already available with this design for risk reduction (Refs. 47 to 50).

Neutralizer keeper voltage, relative to neutralizer cathode common, and the coupling voltage between neutralizer cathode common and the vacuum facility ground are shown in Figure 10. The keeper voltage demonstrated a slight decrease over 19.5 kh during which it was operated at fixed emission current and flow rate (Ref. 24). The neutralizer keeper voltage decreased from 11.2 to 10.7 V during the first 10 kh at full-power. This minor decrease is likely due to erosion of the neutralizer cathode orifice plate. The application of a two-dimensional axisymmetric model of the plasma and neutral gas in electric propulsion hollow cathodes for the NEXT LDT neutralizer reveals that the anticipated erosion of the cathode orifice channel is sufficient to cause the observed keeper voltage drop with time (Ref. 51). While in-situ cameras image the minimum neutralizer orifice diameter, detailed erosion orifice channel profile data cannot be determined using the NEXT LDT cameras. Post-test measurements will be made. A decreasing nominal keeper voltage of similar magnitude was observed at full-power during the NSTAR ELT as well (Refs. 32 and 36). The observed neutralizer keeper voltage variability of ± 0.25 V for fixed operating conditions is considerably less than those observed in NSTAR ELT neutralizer cathode where the variations on the order of a volt are evident in the keeper voltage (Refs. 32 and 36). The NEXT coupling voltage was steady at –10.2 V ± 0.2 V during the first 19.5 kh. Spikes in the keeper and coupling voltages are due to thruster shutdown and restart events where steady-state conditions do not exist for the neutralizer. There have been 226 neutralizer ignitions all within 6 min of application of the heater current. Typical ignition durations are between 3.5 to 4.0 min (Ref. 40). The main observed neutralizer degradation is the loss of flow margin with testing duration and will be discussed later.

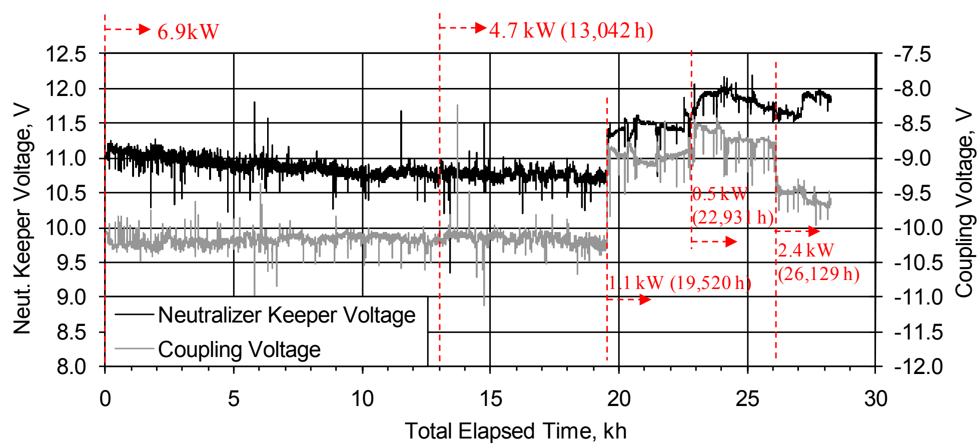

Figure 10.—NEXT LDT neutralizer keeper and coupling voltage data as a function of time.

Accelerator Grid

The performance of the ion optics has exceeded pretest expectations. An initial decrease in accelerator current was observed at the beginning of the test due to burn-in of the ion optics, BOL accelerator grid erosion—primarily restricted to outer radii accelerator grid aperture enlargement for NEXT (Ref. 24). The overall trend since has been a slight decrease in observed accelerator currents as the downstream diameter of the apertures erode, shown in Figure 11. The accelerator current for the NSTAR thruster on DS1 was ~25 percent less in space than the NSTAR data obtained during preflight measurements in a test facility operating with an operating background pressure of 3.5×10^{-6} Torr (Refs. 2, 36, and 41). Because the NEXT LDT is operating in comparable, yet slightly higher operating background pressures, it is expected that the NEXT accelerator current in space would be reduced by ≥25 percent compared to those measured in this test facility. Decreased background pressures in space reduce charge-exchange ion production.

Electron backstreaming and perveance margins throughout the wear test are plotted in Figure 12 and Figure 13, respectively. Electron backstreaming limit, impingement-limited total voltage (perveance limit), and screen grid ion transparency measurement techniques are defined in Reference 52. Electron backstreaming margin has been relatively constant for all operating conditions over the entire test duration; however, a slightly increasing trend is discernable. At full-power, the electron backstreaming margin has improved by ~5 V since the beginning of the test. The backstreaming margin has been observed to decrease slightly following perveance measurements indicating the cause of the improved margin may be the result of backsputtered deposition on the accelerator cusps, which is removed when the beamlets are defocused during perveance measurements. The source of the backsputtered material, evident from in-situ images, is carbon from the beam dump and vacuum facility walls due to the high-energy ion beam impingement. This behavior is an artifact of ground testing and would not be observed in space.

The NSTAR first failure mode is electron backstreaming, encountered after 25,700 h (211 kg throughput), preventing full-power operation (Ref. 36). The NSTAR ELT full-power electron backstreaming limit increased in magnitude by 100 V from the beginning-of-test value to the ultimate failure after reaching the maximum power processor output of –250 V (i.e., a loss of margin of 100 V (Ref. 36)). The negligible change in the NEXT electron backstreaming margin (a few volts) demonstrates that the NSTAR first failure mode has been mitigated by the improved, second-generation NEXT design.

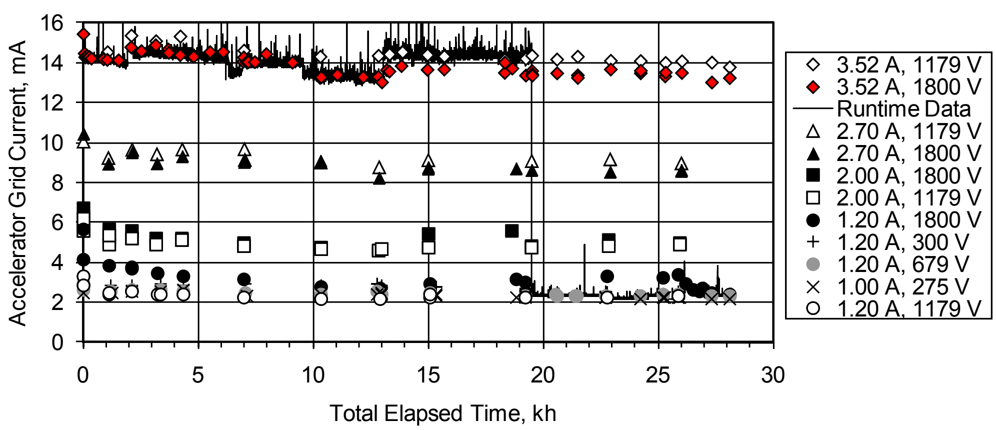

Figure 11.—NEXT LDT accelerator grid current data as a function of time.

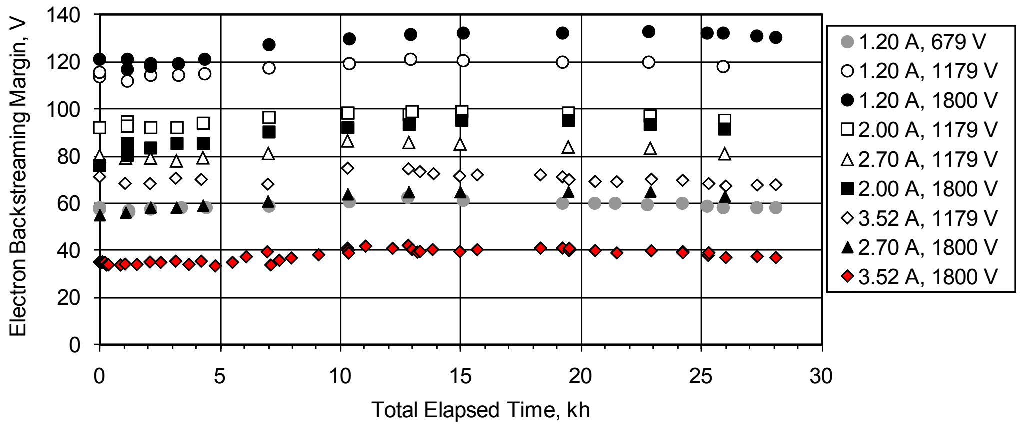

Figure 12.—NEXT LDT electron backstreaming margin data as a function of time.

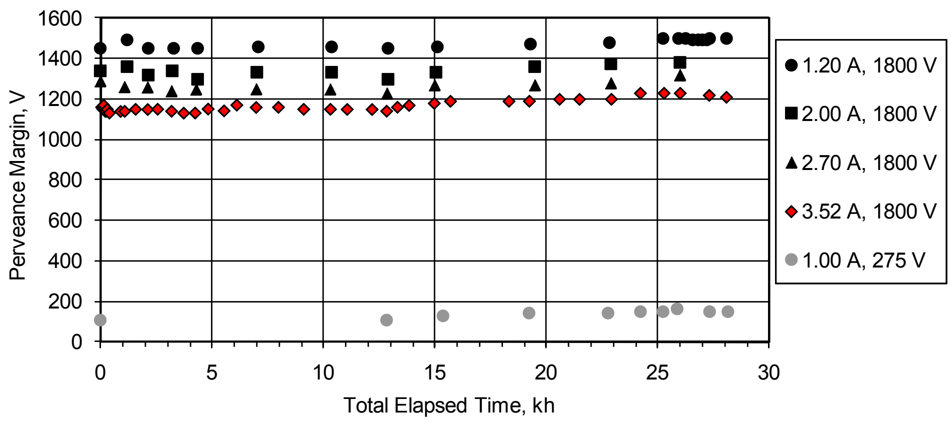

Figure 13.—NEXT LDT perveance margin data as a function of time.

Perveance margins have increased as expected due to the downstream erosion (chamfering) of the accelerator apertures. Similar increases in perveance margin were observed during the NSTAR ELT (Ref. 36). Screen grid ion transparencies exhibited a slight decrease of a few percentage points during the first 10 kh. Screen grid ion transparency data can be found in Reference 22. Changes in electron backstreaming limit, perveance limit, and screen grid ion transparencies are not significant enough to degrade the ion optics' performance and are less than or equal to those exhibited by the NSTAR ion optics during the 8,200 h wear test and NSTAR ELT (Refs. 30 and 32).

NEXT LDT Erosion Data

Erosion of critical thruster components has been within modeling predictions and consistent with the NEXT service life assessment (Refs. 16, 17, and 23). Several of the NSTAR ELT-observed wear anomalies have been significantly reduced or eliminated. There has not been observed discharge cathode keeper orifice erosion. There has not been a measured increase in accelerator grid aperture cusp diameters except for at the outer edge. There has not been a measured change in the cold grid-gap of the ion optics for the NEXT engine. The above three wear characteristics were observed during the NSTAR ELT of the DS1 flight spare (Ref. 36). The accelerator aperture cusp enlargement and reduction in optics' grid gap led to the first failure of the NSTAR thruster—inability to prevent electron backstreaming. By eliminating these two wear mechanisms through improved NEXT design and operating characteristics, the NSTAR first failure has been mitigated.

The erosion of the accelerator grid of the ion optics due to charge-exchange ions is the predicted life limiter of the NEXT thruster for all operating conditions. The charge-exchange ions erode the accelerator grid in a pit and groove hexagonal pattern. Eventually, the groove depth will increase until it penetrates the accelerator grid thickness, which can lead to the loss of accelerator gird structural integrity. This erosion is being quantified through in-situ measurements during the LDT for multiple operating conditions spanning the broad range of the NEXT throttle table. These measurements, among many others, are being used to validate the thruster service life model.

Discharge and Neutralizer Cathodes

The NSTAR ELT uncovered previously unknown failure modes relating to both the discharge and neutralizer cathodes. The severe erosion of the discharge cathode assembly (DCA) in the ELT led to the complete removal of the keeper faceplate, exposing the discharge cathode and heater to eroding ions. This erosion was preceded by a keeper-to-cathode-common short that likely exacerbated this erosion. Additional failure modes were uncovered during the NSTAR ELT resulting from erosion of the DCA (Ref. 36). These failure modes are: the inability to ignite the DCA due to the keeper short, breaching of the heater sheath due to excessive erosion after the keeper faceplate is removed, and ion optics failures (either due to unclearable shorting or rogue hole formation) resulting from erosion of the DCA radiation shield causing large flakes to break free (Ref. 36).

Throughout the NEXT LDT, an in-situ camera has been used to document the erosion of the DCA. Figure 14 shows images of the NEXT LDT discharge cathode assembly. The primary function of the discharge cathode keeper is to protect the discharge cathode from excessive sputter erosion. The EM3 keeper material was changed to graphite following the 2,000 h NEXT wear test, which has a sputter yield 1/20 than that of molybdenum at 50 eV (Ref. 33). Scaling the NEXT 2,000 h wear test molybdenum discharge keeper erosion rate (depth of 17 percent of the keeper thickness after test) with the decrease in sputter yield of graphite compared to molybdenum gives a conservative estimate of wear through of the keeper after > 87 kh at full-power (or >1800 kg) (Refs. 25, 33, and 53). There has been no observed erosion of the NEXT DCA in the orifice inner diameter, the keeper inner diameter, or the keeper outer diameter. The data, shown in Figure 15, indicate the negligible change in critical dimensions of the NEXT DCA.

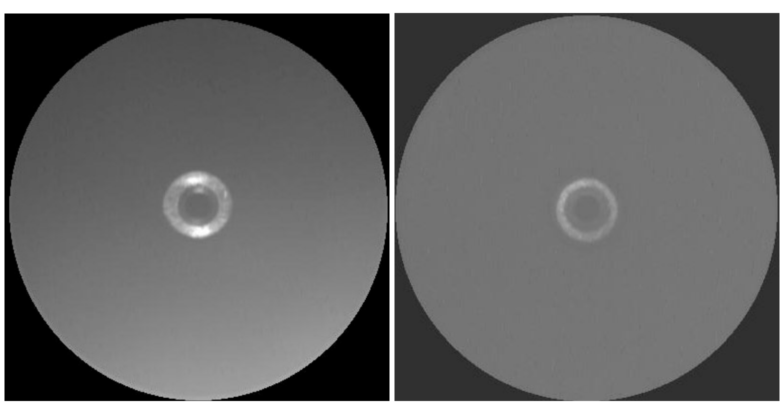

Figure 14.—NEXT LDT discharge cathode assembly BOL (left) and after 28,122 h (right).

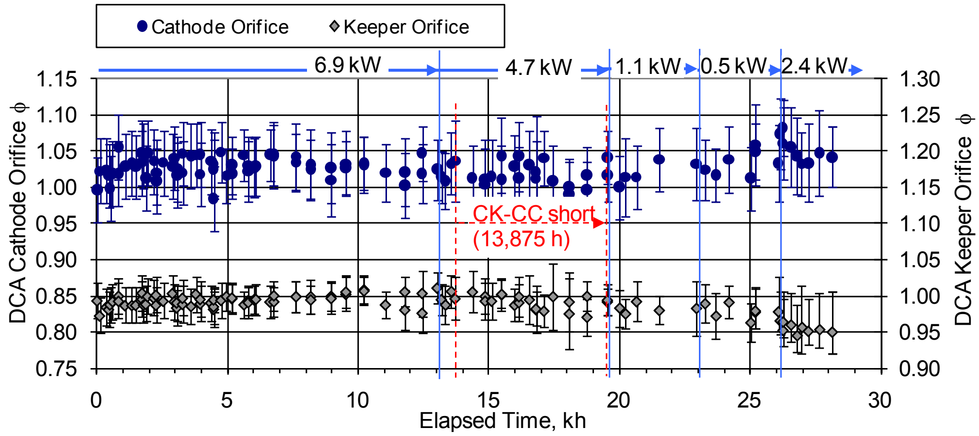

Figure 15.—NEXT LDT DCA non-dimensional data as a function of time.

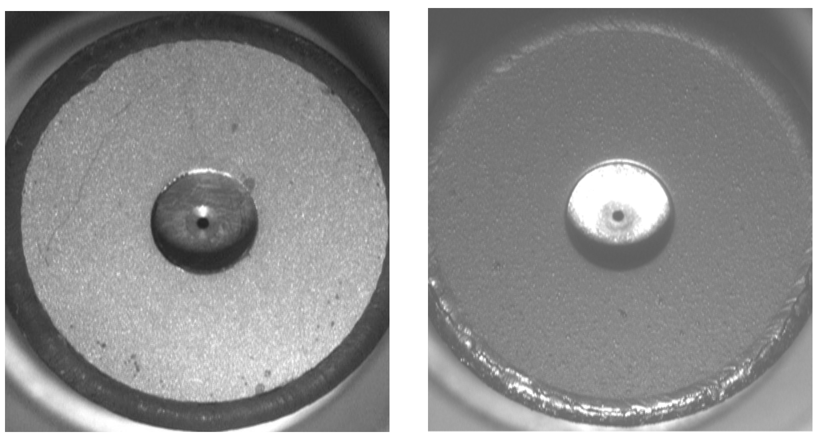

Figure 16.—NEXT LDT neutralizer cathode assembly BOL (left) and after 28,122 h (right).

Two failure modes relating to the neutralizer cathode assembly (NCA) that the NSTAR ELT highlighted were loss of flow margin resulting in plume-mode operation and orifice clogging due to low-temperature operation (Ref. 36). It is well understood that operation of the neutralizer cathode in a regime where there are large peak-to-peak components of voltage and current, known as plume-mode, can lead to excessive wear of the neutralizer. A loss of neutralizer flow margin, defined as the difference between set point and onset of plume-mode, was observed during the NSTAR ELT at low-power leading to a change in the input parameters to the thruster for this condition for the Dawn mission (Refs. 36, 54, and 55). While a loss of flow margin was observed for full-power operation, the cause of the loss of flow margin at low-power was orifice clogging. The temperature-dependent orifice-clogging resulted in complete loss of flow margin at low-power (Ref. 36).

Observed erosion of the NEXT LDT neutralizer has been minimal, as is shown in Figure 16. Measured orifice data are displayed in Figure 17. Critical dimensions such as the inner diameter of the cathode orifice and keeper orifice have demonstrated no change over the test duration. Based upon other wear tests, it is expected that the orifice channel geometry is changing, but the camera only measures the minimum diameter (Refs. 30 and 36). No clogging has been observed, which is most important for the low-power operating conditions.

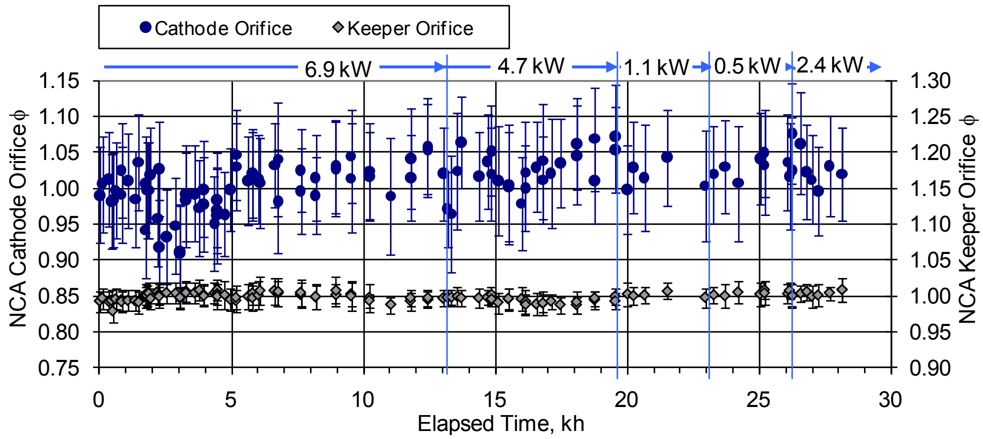

Figure 17.—NEXT LDT neutralizer cathode non-dimensional data as a function of time.

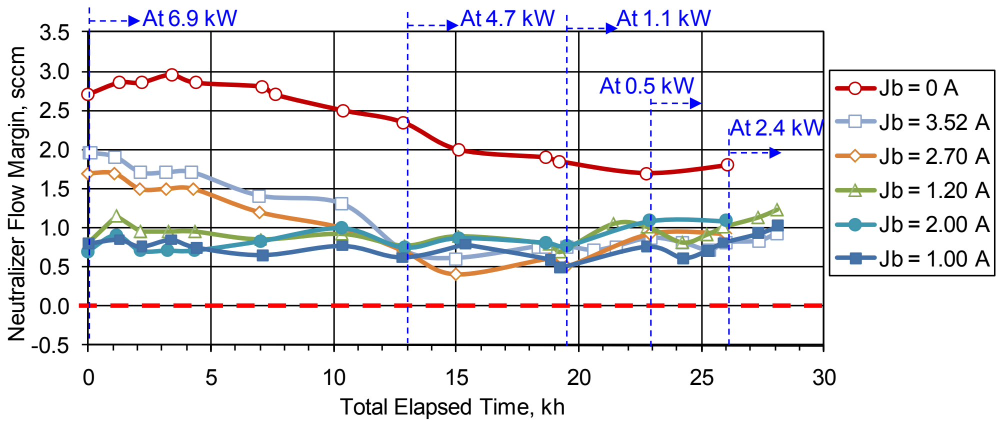

Figure 18.—Anticipated NEXT PM neutralizer flow margin data as a function of time operated in the NEXT LDT throttling profile. Measurement error is ± 0.1 sccm.

Relative to the NEXT technology development throttle table at the inception of the NEXT LDT, a loss in neutralizer flow margin had been observed. Transition flow margin has decreased, based on BOL neutralizer flow rates, for all beam current conditions over the test duration (Ref. 40). Motivated by the EM neutralizer low flow margin at BOL, design modifications have been incorporated into the PM neutralizer design yielding higher flow margin at low-power (Ref. 8). The design changes caused a slight decrease in PM neutralizer flow margin at high emission current where substantial BOL margin exits. The PM neutralizer design change also results in an approximate one volt increase in the magnitude of the coupling voltage (Ref. 8). A new throttle table (TT10) was released to address the observed degradation experienced during the LDT and is now the baseline throttle table for the technology program and for mission analyses (Ref. 40). The new throttle table, defined in Table 3 and Table 4 of the Appendix, increases the neutralizer flow rate from beginning of life as a function of propellant throughput processed. To determine neutralizer flow margin for a flight thruster utilizing a PM neutralizer, the LDT data was shifted based upon the difference between the pretest characterization data from the EM3 neutralizer and two PM neutralizers (Refs. 8, 19, and 40). This resulted in a shift up in flow margin of the LDT data at low power of up to 0.5 sccm and a shift down at full-power by 0.3 sccm. Figure 18 shows the predicted flow margin of a flight-like neutralizer operated in the NEXT LDT throttling profile. The flow set points, used to calculate flow margins, are from TT10. As the figure illustrates, there would have been positive flow margin of at least 0.4 sccm for all operating conditions throughout the NEXT LDT had it utilized a PM neutralizer and updated TT10 neutralizer flow rate inputs.

Accelerator Grid

The inability to prevent electron backstreaming at full-power was the first failure mode encountered during the NSTAR ELT (Ref. 36). Charge-exchange ions impinge upon the downstream surface eroding the barrel of the accelerator grid apertures, the downstream edge (causing a chamfer) of the apertures, and cause the pit and groove erosion pattern on the downstream surface of the accelerator grid. Charge-exchange ion production is greater in regions of high ion current and neutral densities. This occurs along thruster centerline for most ion thrusters due to the peaked beam current density there. Thus, the most severe charge-exchange erosion for the NEXT thruster occurs at the center radius aperture where the beam current density is highest (Ref. 23).

The failure to prevent electron backstreaming, after increasing the power supply voltage from the throttle table setpoint of -180 V to the maximum flight power-processor unit accelerator voltage of –250 V, was reached after 25,700 h of operation (211 kg of xenon) during the NSTAR ELT (Refs. 15, 36, and 56). The thruster was fully functional at lower throttle levels and was operated for another 4,652 h prior to voluntary termination (Ref. 36). In-situ cameras are used to document the minimum diameter and downstream chamfer dimension of the accelerator apertures at various radial locations during the NEXT LDT. The primary location of interest for electron backstreaming is the center radius aperture. There has been no cusp enlargement observed during the NEXT LDT at the centerline location, which caused the NSTAR ELT first failure mode. The reason for the lack of significant aperture enlargement, other than downstream chamfering, is primarily a result of a flatter beam current density profile, highly focused beamlets, and a larger BOL aperture diameter for NEXT compared to NSTAR. Figure 19 shows the critical dimensions of the centerline aperture of the accelerator grid during the NEXT LDT and NSTAR ELT, normalized to BOL dimensions. There is a lack of cusp enlargement for reasons previously described. There has also been minimal downstream chamfer erosion, between a 5 to 10 percent increase over the testing duration. The discrepancy in two sets of data obtained most recently are due to movement of the thruster axially to intentionally improve the image quality (i.e., focus) while obtaining the images. This resulted in a decrease in the observed diameters for the cusp and the downstream diameter because the edges are more clearly defined. As such, the increased downstream diameter for the NEXT LDT is likely overestimated.

Negligible erosion of the aperture cusps is the reason that negligible electron backstreaming margin change has occurred. Thus, the NSTAR first failure mode has been mitigated by the improved NEXT beam flatness and other design/operational improvements.

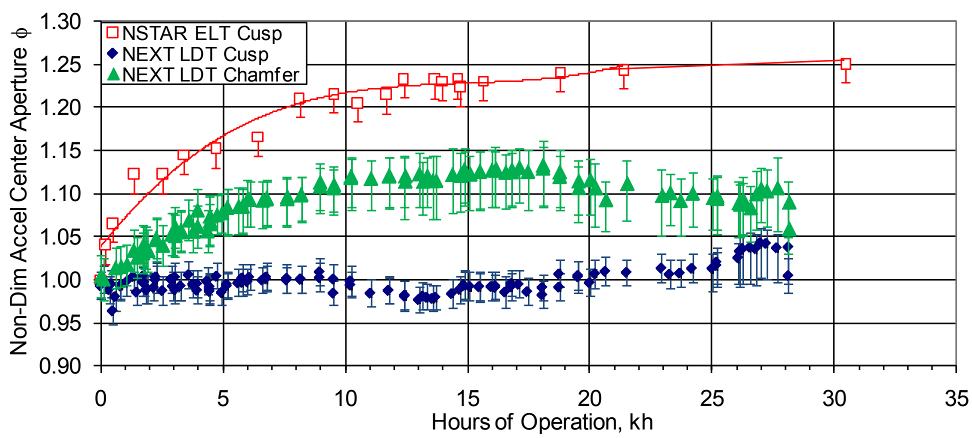

Figure 19.—NEXT and NSTAR centerline accelerator grid aperture data.

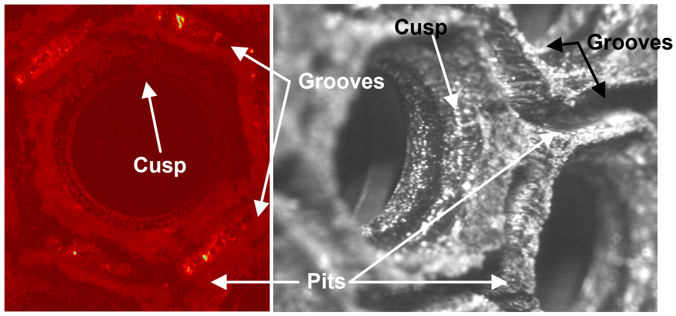

Figure 20.—NEXT LDT accelerator grid center radius aperture after 28,122 h.

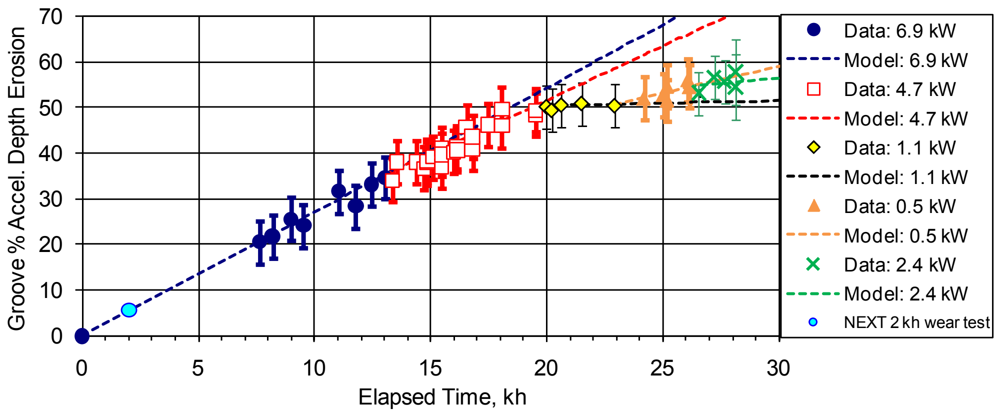

Figure 21.—NEXT centerline accelerator grid groove penetration depth data.

Having addressed the NSTAR first wear-out mode through the NEXT thruster design, another wear-out mode has moved to the forefront. The NEXT first failure mode is predicted to be pit and groove erosion due to charge-exchange erosion (Ref. 16 and 17). During the post-test thruster inspection from the NSTAR ELT, through-pits were observed within a 7 cm radius of thruster centerline (Ref. 36). After a hole is formed through an accelerator grid, undercutting is caused on the grid upstream surface by ions that were repelled by the intra-grid electric field after passing through the pit (Ref. 36). The pit-and-groove erosion pattern at thruster centerline has been monitored by an in-situ camera during the NEXT LDT, with most recent images shown in Figure 20. At full power, there were no observed pits forming at centerline for the NEXT thrusters. Pits were clearly evident after operation of the thruster at the second throttled condition, 4.7 kW input power.

The groove penetration rate has been measured and monitored at each of the operating conditions by a technique that utilizes the curvature of the domed accelerator grid, the radial translation stage, and depth-of-field of the camera (Ref. 57). The data show excellent agreement with the groove depth model that was used during the thruster service life assessment, illustrated in Figure 21 (Refs. 16 and 17). Validation of the model for groove penetration (i.e., the predicted first wear-out mode for the NEXT thruster) has been achieved at five different operating conditions that span the NEXT thruster throttling range, incorporate the conditions with the highest groove erosion rate, and encompass the boundary operating conditions of the NEXT throttle table. Both the modeling results and measured data indicate that the groove erosion rate, as a function of operating time, is the highest for full-power operation. Extrapolation of groove depth until penetration through the accelerator grid at full-power gives a minimum thruster service life of 36 kh, which corresponds to processing 750 kg of xenon.

The usable thruster service life will extend beyond this minimum operating time if the mission application operates for any appreciable time at operating conditions other than full-power where the groove erosion rate is lower. This is the most probable mission application as the NEXT IPS was designed for solar electric propulsion that would see a throttling down in power as the outbound mission trajectory causes a decrease in solar flux and thus available power for the propulsion system. Following the throttling plan outlined in Table 1, the current plan is to operate the thruster at full-power, the highest groove erosion rate, until failure. It is predicted that the thruster will reach wear through of the grooves after 45 kh and processing 800 kg if operated in this manner. This throttling scheme is very aggressive and would have operated for 64 percent of the operating duration at the worst groove erosion rate condition, full-power. It is likely that considerable time would be spent operating at conditions other than full-power for mission applications. To assess thruster service life for mission applications, a service life assessment needs to be conducted using the validated service model tools with the anticipated mission throttling scheme as an input as outlined in the thruster lifetime qualification standard (Refs. 15 and 56).

Two unavoidable impacts of ground-based thruster lifetime testing are the increased accelerator currents due to higher operating background pressures resulting from finite facility pumping speeds and backsputtered material from the vacuum facility walls. As stated previously based upon NSTAR accelerator currents in-space compared to ground based testing, it is expected that the NEXT in-space accelerator current would be reduced by $\geq$25 percent compared to those measured in this test facility. As a result, the charge-exchange erosion and subsequent pit-and-groove erosion would be decreased by a corresponding amount.

Application of a model developed to predict the effect of back-sputtering on grid erosion, with a 3 μm/kh back-sputter rate at full-power and center-radius aperture ion impingement current density, estimates a maximum of 10 percent reduction in erosion near the beam center, where pit and groove erosion rate is highest, during the NEXT LDT due to backsputtered carbon (Ref. 58). Additional analyses have been performed to predict the impact of the backsputtered carbon deposition on the accelerator grid utilizing the MICHELLE particle-in-cell code (Ref. 59). The resulting analysis estimates a 30 percent reduction in the maximum groove erosion due to carbon deposition in the LDT (Ref. 59). The combined effects of elevated background pressure in the test facility and backsputtered carbon deposition essentially cancel out and therefore the LDT groove wear is anticipated to be representative of thruster operation in space.

Summary and Conclusions

As of April 5, 2010, the NEXT EM3 thruster has accumulated 28,500 h of operation. The NEXT thruster has processed 466 kg of xenon; *nearly double the total propellant throughput processed by the DS1 flight spare in the NSTAR ELT (235 kg)*. NEXT project qualification throughput of 450 kg was demonstrated in December 2009 satisfying the original main goal of the NEXT LDT. The main testing objective has been changed to test the thruster to failure. The NEXT thruster has demonstrated a total impulse of 17 MN·s to date; *the highest total impulse ever demonstrated by an ion thruster and the highest total impulse ever demonstrated by any sub-100 kW electric propulsion device*.

Overall thruster performance, which includes thrust, input power, specific impulse, and thrust efficiency, has negligible signs of degradation. Performance of the discharge cathode, discharge chamber, and ion optics have been within pretest predictions demonstrating limited degradation and less variation compared to that observed during the NSTAR ELT. The only source of non-negligible thruster performance degradation has been the loss neutralizer flow margin with accumulated throughput and has been addressed by a design change in the prototype-model neutralizer and updated NEXT throttle table. Erosion rates of the critical thruster components that experienced severe erosion during the NSTAR ELT such as the discharge cathode assembly and accelerator aperture cusps have been negligible. The improved NEXT design attributes as a second generation ion thruster have successfully mitigated the NSTAR first wear-out mode (i.e., accelerator barrel erosion leading to inability to prevent electron backstreaming). The NEXT first wear-out mode is predicted to be wear through of accelerator grooves leading to the eventual loss of structural integrity. Progression of the groove penetration depth has been measured at five operating conditions validating the groove penetration model. Extrapolation of the groove erosion rate to wear through indicates a *minimum* thruster service life of 27 kh (corresponding to 750 kg throughput) at the worst groove erosion rate condition—full-power. Additional collected data are used to validate the thruster service life assessment tools.

A trajectory-specific thruster lifetime assessment can be made using the validated thruster service life models consistent with the electric thruster lifetime qualification standard (Ref. 15). Given the intended plan for continued thruster operation for the NEXT LDT, grove penetration is predicted after 45 kh (corresponding to 800 kg throughput) with highly aggressive throttling scheme that operates at full-power for 64 percent of the operating time.

Appendix

TABLE 3.—NEXT BOL THROTTLE TABLE (TT10) WITH LDT PERFORMANCE OPERATING CONDITIONS SUBSET SHADED. FULL-POWER WEAR TEST CONDITION IN BOLD

TL Level	P_{IN}, kW[†]	J_B, A	V_B, V	V_A, V	m_M, sccm	m_C, sccm	m_N, sccm	J_{NK}, A
40	**6.86**	**3.52**	**1800**	**–210**	**49.6**	**4.87**	**4.01**	**3.00**
39	6.05	3.52	1570	–210	49.6	4.87	4.01	3.00
38	5.46	3.52	1400	–210	49.6	4.87	4.01	3.00
37	4.71	3.52	1180	–200	49.6	4.87	4.01	3.00
36	6.06	3.10	1800	–210	43.5	4.54	4.01	3.00
35	5.35	3.10	1570	–210	43.5	4.54	4.01	3.00
34	4.82	3.10	1400	–210	43.5	4.54	4.01	3.00
33	4.14	3.10	1180	–200	43.5	4.54	4.01	3.00
32	5.29	2.70	1800	–210	37.6	4.26	3.50	3.00
31	4.67	2.70	1570	–210	37.6	4.26	3.50	3.00
30	4.22	2.70	1400	–210	37.6	4.26	3.50	3.00
29	3.64	2.70	1180	–200	37.6	4.26	3.50	3.00
28	3.22	2.70	1020	–175	37.6	4.26	3.50	3.00
27	4.62	2.35	1800	–210	32.4	4.05	3.50	3.00
26	4.08	2.35	1570	–210	32.4	4.05	3.50	3.00
25	3.68	2.35	1400	–210	32.4	4.05	3.50	3.00
24	3.18	2.35	1180	–200	32.4	4.05	3.50	3.00
23	2.82	2.35	1020	–175	32.4	4.05	3.50	3.00
22	4.01	2.00	1800	–210	25.8	3.87	2.50	3.00
21	3.54	2.00	1570	–210	25.8	3.87	2.50	3.00
20	3.21	2.00	1400	–210	25.8	3.87	2.50	3.00
19	2.78	2.00	1180	–200	25.8	3.87	2.50	3.00
18	2.47	2.00	1020	–175	25.8	3.87	2.50	3.00
17	3.25	1.60	1800	–210	20.0	3.70	2.75	3.00
16	2.88	1.60	1570	–210	20.0	3.70	2.75	3.00
15	2.61	1.60	1400	–210	20.0	3.70	2.75	3.00
14	2.27	1.60	1180	–200	20.0	3.70	2.75	3.00
13	2.02	1.60	1020	–175	20.0	3.70	2.75	3.00
12	2.44	1.20	1800	–210	14.2	3.57	3.00	3.00
11	2.16	1.20	1570	–210	14.2	3.57	3.00	3.00
10	1.96	1.20	1400	–210	14.2	3.57	3.00	3.00
9	1.70	1.20	1180	–200	14.2	3.57	3.00	3.00
8	1.52	1.20	1020	–175	14.2	3.57	3.00	3.00
7	1.42	1.20	936	–150	14.2	3.57	3.00	3.00
6	1.32	1.20	850	–125	14.2	3.57	3.00	3.00
5	1.12	1.20	679	–115	14.2	3.57	3.00	3.00
4	1.09	1.20	650	–144	14.2	3.57	3.00	3.00
3	0.789	1.20	400	–310	14.2	3.57	3.00	3.00
2	0.669	1.20	300	–410	14.2	3.57	3.00	3.00
1	0.545	1.00	275	–350	12.3	3.52	3.00	3.00

[†] Nominal values at beginning of life.

TABLE 4.—NEXT THROTTLE TABLE (TT10) NEUTRALIZER FLOW RATE SET POINT AS A FUNCTION OF PROPELLANT THROUGHPUT FOR FIXED NEUTRALIZER KEEPER CURRENT OF 3.00 A. NEXT LDT PERFORMANCE OPERATING CONDITIONS SUBSET SHADED. FULL-POWER WEAR TEST CONDITION IN BOLD. AFTER EACH THROUGHPUT MILESTONE IS SURPASSED, THE NEW FLOW RATE BECOMES THE SET POINT

			Neutralizer flow rate (m_N), sccm					
TL Level	P_{IN}, kW†	J_B, A	0 kg	100 kg	200 kg	300 kg	400 kg	450 kg
40	**6.86**	**3.52**	**4.01**	**4.01**	**4.01**	**4.01**	**4.01**	**4.33**
39	6.05	3.52	4.01	4.01	4.01	4.01	4.01	4.33
38	5.46	3.52	4.01	4.01	4.01	4.01	4.01	4.33
37	4.71	3.52	4.01	4.01	4.01	4.01	4.01	4.33
36	6.06	3.10	4.01	4.01	4.01	4.01	4.01	4.33
35	5.35	3.10	4.01	4.01	4.01	4.01	4.01	4.33
34	4.82	3.10	4.01	4.01	4.01	4.01	4.01	4.33
33	4.14	3.10	4.01	4.01	4.01	4.01	4.01	4.33
32	5.29	2.70	3.50	3.50	3.50	3.50	3.82	4.14
31	4.67	2.70	3.50	3.50	3.50	3.50	3.82	4.14
30	4.22	2.70	3.50	3.50	3.50	3.50	3.82	4.14
29	3.64	2.70	3.50	3.50	3.50	3.50	3.82	4.14
28	3.22	2.70	3.50	3.50	3.50	3.50	3.82	4.14
27	4.62	2.35	3.50	3.50	3.50	3.50	3.82	4.14
26	4.08	2.35	3.50	3.50	3.50	3.50	3.82	4.14
25	3.68	2.35	3.50	3.50	3.50	3.50	3.82	4.14
24	3.18	2.35	3.50	3.50	3.50	3.50	3.82	4.14
23	2.82	2.35	3.50	3.50	3.50	3.50	3.82	4.14
22	4.01	2.00	2.50	2.82	3.14	3.46	3.78	4.10
21	3.54	2.00	2.50	2.82	3.14	3.46	3.78	4.10
20	3.21	2.00	2.50	2.82	3.14	3.46	3.78	4.10
19	2.78	2.00	2.50	2.82	3.14	3.46	3.78	4.10
18	2.47	2.00	2.50	2.82	3.14	3.46	3.78	4.10
17	3.25	1.60	2.75	3.00	3.32	3.64	3.96	4.28
16	2.88	1.60	2.75	3.00	3.32	3.64	3.96	4.28
15	2.61	1.60	2.75	3.00	3.32	3.64	3.96	4.28
14	2.27	1.60	2.75	3.00	3.32	3.64	3.96	4.28
13	2.02	1.60	2.75	3.00	3.32	3.64	3.96	4.28
12	2.44	1.20	3.00	3.00	3.32	3.64	3.96	4.28
11	2.16	1.20	3.00	3.00	3.32	3.64	3.96	4.28
10	1.96	1.20	3.00	3.00	3.32	3.64	3.96	4.28
9	1.70	1.20	3.00	3.00	3.32	3.64	3.96	4.28
8	1.52	1.20	3.00	3.00	3.32	3.64	3.96	4.28
7	1.42	1.20	3.00	3.00	3.32	3.64	3.96	4.28
6	1.32	1.20	3.00	3.00	3.32	3.64	3.96	4.28
5	1.12	1.20	3.00	3.00	3.32	3.64	3.96	4.28
4	1.09	1.20	3.00	3.00	3.32	3.64	3.96	4.28
3	0.789	1.20	3.00	3.00	3.32	3.64	3.96	4.28
2	0.669	1.20	3.00	3.00	3.32	3.64	3.96	4.28
1	0.545	1.00	3.00	3.00	3.32	3.64	3.96	4.28

† Nominal values at beginning of life.

References

1. Rayman, M.D., The Successful Conclusion of the Deep Space 1 Mission: Important Results Without a Flashy Title," Space Technology, Vol. 23, pp. 185–196, 2003.
2. Polk, J.E., et al., "Performance of the NSTAR Ion Propulsion System on the Deep Space One Mission," AIAA–2001–0965, 39th AIAA Aerospace Sciences Meeting and Exhibit Joint Propulsion Conference, Reno, NV, January 8–11, 2001.
3. Brophy, J.R., Garner, C., and Mikes, S., "Dawn Ion Propulsion System- Initial Checkout after Launch," AIAA–2008–4917, 44th AIAA/ASME/SAE/ASEE Joint Propulsion Conference & Exhibit, Hartford, CT, July 20–23, 2008.
4. Benson, S.W. and Patterson, M.J., "NASAs Evolutionary Xenon Thruster (NEXT) Ion Propulsion Technology Development Status in 2009," IEPC–2009–150, 31st International Electric Propulsion Conference, Ann Arbor, MI, September 20–24, 2009.
5. Cupples, M., Coverstone, V., and Woo, B., "Application of Solar Electric Propulsion to a Comet Surface Sample Return Mission," AIAA–2004–3804, 40th AIAA/ASME/SAE/ASEE Joint Propulsion Conference and Exhibit, Fort Lauderdale, FL, July 11–14, 2004.
6. Benson, S.W., Riehl, J.P., and Oleson, S.R., "NEXT Ion Propulsion System Configurations and Performance for Saturn System Exploration," AIAA–2007–5230, 43rd AIAA/ASME/SAE/ASEE Joint Propulsion Conference and Exhibit, Cincinnati, OH, July 8–11, 2007.
7. Oh, D., Benson, S., Witzberger, K., and Cupples, M., "Deep Space Mission Applications for NEXT: NASA's Evolutionary Xenon Thruster," AIAA–2004–3806, 40th AIAA/ASME/SAE/ASEE Joint Propulsion Conference and Exhibit, Fort Lauderdale, FL, July 11–14, 2004.
8. Herman, D.A., Soulas, G.C., and Patterson, M.J., "Performance Evaluation of the Prototype-Model NEXT Ion Thruster," AIAA–2007–5212 and NASA/TM—2008-215029, 43rd AIAA/ASME/SAE/ASEE Joint Propulsion Conference and Exhibit, Cincinnati, OH, July 8–11, 2007.
9. Pinero, L.R., Todd, P., and Hopson, M., "Integration and Qualification of the NEXT Power Processing Unit," AIAA–2007–5214, 43rd AIAA/ASME/SAE/ASEE Joint Propulsion Conference and Exhibit, Cincinnati, OH, July 8–11, 2007.
10. Patterson, M.J. and Benson, S.W., "NEXT Ion Propulsion System Development Status and Capabilities," Conference Proceedings and NASA/TM—2008-214988, 2007 NASA Science Technology Conference, College Park, MD, June 19–21, 2007.
11. Snyder, J.S., et al., "Vibration Test of a Breadboard Gimbal for the NEXT Ion Engine," AIAA–2006–665, 42nd AIAA/ASME/SAE/ASEE Joint Propulsion Conference and Exhibit, Sacramento, CA, July 9–12, 2006.
12. Aadland, R.S., et al., "Development Status of the NEXT Propellant Management System," AIAA–2004–3974, 40th AIAA/ASME/SAE/ASEE Joint Propulsion Conference and Exhibit, Fort Lauderdale, FL, July 11–14, 2004.
13. Hoskins, W.A., et al., "Development of a Prototype Model Ion Thruster for the NEXT System," AIAA–2004–4111, 40th AIAA/ASME/SAE/ASEE Joint Propulsion Conference and Exhibit, Fort Lauderdale, FL, July 11–14, 2004.
14. Monheiser, J., Aadland, R.S., and Wilson, F., "Development of a Ground Based Digital Control Interface Unit (DCIU) for the NEXT Propulsion System," AIAA–2004–4112, 40th AIAA/ASME/SAE/ASEE Joint Propulsion Conference and Exhibit, Fort Lauderdale, FL, July 11–14, 2004.
15. Dankanich, J.W., Brophy, J.R., and Polk, J.E., "Lifetime Qualification Standard for Electric Thrusters," AIAA–2009–5095, 45th AIAA/ASME/SAE/ASEE Joint Propulsion Conference and Exhibit, Denver, CO, August 2–5, 2009.
16. Van Noord, J.L., "Lifetime Assessment of the NEXT Ion Thruster," AIAA–2007–5274, 43rd AIAA/ASME/SAE/ASEE Joint Propulsion Conference and Exhibit, Cincinnati, OH, July 8–11, 2007.
17. Van Noord, J.L. and Herman, D.A., "Application of the NEXT Ion Thruster Lifetime Assessment to Thruster Throttling," AIAA–2008–4526, 44th AIAA/ASME/SAE/ASEE Joint Propulsion Conference and Exhibit, Hartford, CT, July 21–23, 2008.

18. Soulas, G.C., et al., "NEXT Ion Engine 2000 Hour Wear Test Results," AIAA–2004–3791, 40th AIAA/ASME/SAE/ASEE Joint Propulsion Conference and Exhibit, Fort Lauderdale, FL, July 11–14, 2004.
19. Soulas, G.C. and Patterson, M.J., "NEXT Ion Thruster Performance Dispersion Analyses," AIAA–2007–5213, 43rd AIAA/ASME/SAE/ASEE Joint Propulsion Conference and Exhibit, Cincinnati, OH, July 8–11, 2007.
20. Van Noord, J.L., Soulas, G.C., and Sovey, J.S., "NEXT PM1R Ion Thruster and Propellant Management System Wear Test Results," IEPC–2009–163, 31st International Electric Propulsion Conference, Ann Arbor, MI, September 20–24, 2009.
21. Herman, D.A., Pinero, L.R., and Sovey, J.S., "NASA's Evolutionary Xenon Thruster (NEXT) Component Verification Testing," AIAA–2008–4812, 44th AIAA/ASME/SAE/ASEE Joint Propulsion Conference and Exhibit, Hartford, CT, July 21–23, 2008.
22. Herman, D.A., Soulas, G.C., and Patterson, M.J., "Status of the NEXT Long-Duration Test after 23,300 Hours of Operation," AIAA–2009–4917, 45th AIAA/ASME/SAE/ASEE Joint Propulsion Conference & Exhibit, Denver, CO, August 2–5, 2009.
23. Herman, D.A., Soulas, G.C., and Patterson, M.J., "NEXT Long-Duration Test Plume and Wear Characteristics after 16,550 h of Operation and 337 kg of Xenon Processed," AIAA–2008–4919, 44th AIAA/ASME/SAE/ASEE Joint Propulsion Conference and Exhibit, Hartford, CT, July 21–23, 2008.
24. Herman, D.A., Soulas, G.C., and Patterson, M.J., "Performance Characteristics of the NEXT Long-Duration Test after 16,550 h and 337 kg of Xenon Processed," AIAA–2008–4527, 44th AIAA/ASME/SAE/ASEE Joint Propulsion Conference and Exhibit, Hartford, CT, July 21–23, 2008.
25. Kamhawi, H., Soulas, G.C., and Patterson, M., "NEXT Ion Engine 2000 hour Wear Test Plume and Erosion Results," AIAA–2004–3792, 40th AIAA/ASME/SAE/ASEE Joint Propulsion Conference and Exhibit, Fort Lauderdale, FL, July 11–14, 2004.
26. Patterson, M.J. and Benson, S.W., "NEXT Ion Propulsion System Development Status and Performance," AIAA–2007–5199, 43rd AIAA/ASME/SAE/ASEE Joint Propulsion Conference and Exhibit, Cincinnati, OH, July 8–11, 2007.
27. Soulas, G.C., Domonkos, M.T., and Patterson, M.J., "Performance Evaluation of the NEXT Ion Engine," AIAA–2003–5278, 39th AIAA/ASME/SAE/ASEE Joint Propulsion Conference and Exhibit, Huntsville, AL, July 20–23, 2003.
28. Patterson, M.J., et al., "NEXT: NASA's Evolutionary Xenon Thruster," AIAA–2002–3832, 38th AIAA/ASME/SAE/ASEE Joint Propulsion Conference and Exhibit, Indianapolis, IN, July 7–10, 2002.
29. Frandina, M.M., et al., "Status of the NEXT Ion Thruster Long Duration Test," AIAA–2005–4065, 41st AIAA/ASME/SAE/ASEE Joint Propulsion Conference and Exhibit, Tucson, AZ, July 10–13, 2005.
30. Polk, J.E., et al., "An Overview of the Results from an 8200 Hour Wear Test of the NSTAR Ion Thruster," AIAA–1999–2446, 35th AIAA/ASME/SAE/ASEE Joint Propulsion Conference and Exhibit, Los Angeles, CA, June 20–24, 1999.
31. Polk, J.E., et al., "A 1000 Hour Wear Test of the NASA NSTAR Ion Thruster," AIAA–1996–2784, 32nd AIAA/ASME/SAE/ASEE Joint Propulsion Conference and Exhibit, Lake Buena Vista, FL, July 1–3, 1996.
32. Sengupta, A., et al., "An Overview of the Results from the 30,000 Hr Life Test of Deep Space 1 Flight Spare Engine," AIAA–2004–3608, 40th AIAA/ASME/SAE/ASEE Joint Propulsion Conference and Exhibit, Fort Lauderdale, FL, July 11–14, 2004.
33. Doerner, R.P., Whyte, D.G., and Goebel, D.M., "Sputtering Yield Measurements during Low Energy Xenon Plasma Bombardment," Journal of Applied Physics, Vol. 93, No. 9, pp. 5816–5823, May 1, 2003.
34. Brophy, J.R., et al., "The Ion Propulsion System for Dawn," AIAA–2003–4542, 39th AIAA/ASME/SAE/ASEE Joint Propulsion Conference and Exhibit, Huntsville, AL, July 20–23, 2003.

35. Brophy, J.R., et al., “Status of the Dawn Ion Propulsion System,” AIAA–2004–3433, 40th AIAA/ASME/SAE/ASEE Joint Propulsion Conference and Exhibit, Fort Lauderdale, FL, July 11–14, 2004.
36. Sengupta, A., et al., “The 30,000-Hour Extended-Life Test of the Deep Space 1 Flight Spare Ion Thruster,” NASA/TP—2004-213391, NASA Jet Propulsion Laboratory and Glenn Research Center, Pasadena, CA, March 2005.
37. Myers, R.M., “Proceedings of the Nuclear Electric Propulsion Workshop, Volume 1: Introductory Material and Thruster Concepts, Section: “MPD Thruster Technology”,” JPL D–9512 Vol. 1, June 19–22, 1990.
38. Soulas, G.C., “Design and Performance of 40cm Ion optics,” IEPC–01–090, 27th International Electric Propulsion Conference, Pasadena, CA, October 15–19, 2001.
39. Patterson, M.J., Haag, T.W., and Hovan, S.A., “Performance of the NASA 30 cm Ion thruster,” IEPC Paper 93–108, 23rd International Electric Propulsion Conference, Seattle, WA, September 13–16, 1993.
40. Herman, D.A., Soulas, G.C., and Patterson, M.J., “NEXT Long-Duration Test Neutralizer Performance and Erosion Characteristics,” IEPC–2009–154, 31st International Electric Propulsion Conference, Ann Arbor, MI, September 20–24, 2009.
41. Anderson, J.R., et al., “Results of an On-going Long Duration Ground Test of the DS1 Flight Spare Ion Engine,” AIAA–1999–2857, 35th AIAA/ASME/SAE/ASEE Joint Propulsion Conference and Exhibit, Los Angeles, CA, June 20–24, 1999.
42. Anderson, J.R., et al., “Performance Characteristics of the NSTAR Ion Thruster During an On-Going Long Duration Ground Test,” 2000 IEEE Aerospace Conference Proceedings, Vol. 4, pp. 123–148, March 2000.
43. Williams, G.J., “High-Power Electric Propulsion (HiPEP) 2,000-Hour Post-Test Report,” NEXT Internal Report, NASA Glenn Research Center, Cleveland, OH, September 2006.
44. Britton, M., Soulas, G.C., Kamhawi, H., and Snyder, A., “Destructive Analysis of the NEXT 2000-Hour Wear Test Hollow Cathode Assemblies,” NASA/TM—2005-213387, NASA Glenn Research Center, Cleveland, OH, July 2005.
45. Williams, G.J., et al., “Results of the 2000 hr Wear Test of the HiPEP Ion Thruster with Pyrolitic Graphite Ion Optics,” AIAA–2006–4668, 42nd AIAA/ASME/SAE/ASEE Joint Propulsion Conference and Exhibit, Sacramento, CA, July 9–12, 2006.
46. Patterson, M.J., et al., “Plasma Contactor Development for Space Station,” IEPC Paper 93–246, 23rd International Electric Propulsion Conference, Seattle, WA, September 13–16, 1993.
47. Kamhawi, H. and Patterson, M.J., “Update on the Operation Status of the International Space Station Plasma Contactor Hollow Cathode Assemblies,” AIAA–2007–5190, 43rd AIAA/ASME/SAE/ASEE Joint Propulsion Conference and Exhibit, Cincinnati, OH, July 8–11, 2007.
48. Carpenter, C.B., “On the Operational Status of the ISS Plasma Contactor Hollow Cathodes,” AIAA–2004–3425, 40th AIAA/ASME/SAE/ASEE Joint Propulsion Conference and Exhibit, Fort Lauderdale, FL, July 11–14, 2004.
49. Kovaleski, S.D., Patterson, M.J., Soulas, G.C., and Sarver-Verhey, T.R., “A Review of Testing of Hollow Cathodes for the International Space Station Plasma Contactor,” IEPC–2001–271, 27th International Electric Propulsion Conference, Pasadena, CA, October 15–19, 2001.
50. Sarver-Verhey, T.R., “28,000 hour Xenon Hollow Cathode Life Test Results,” NASA CR–206231 and IEPC Paper 97–0168, 25th International Electric Propulsion Conference, Cleveland, OH, August 24–28, 1997.
51. Mikellides, I., et al., “Neutralizer Hollow Cathode Simulations and Comparisons with Ground Test Data,” IEPC–2009–20, 31st International Electric Propulsion Conference, Ann Arbor, MI, September 20–24, 2009.
52. Soulas, G.C., Foster, J.E., and Patterson, M.J., “Performance of Titanium Optics on a NASA 30 cm Ion Thruster,” AIAA–2000–3814, 36th AIAA/ASME/SAE/ASEE Joint Propulsion Conference and Exhibit, Huntsville, AL, July 16–19, 2000.

53. Doerner, R.P. and Goebel, D.M., “Sputtering Yields of Ion Thruster Grid and Cathode Materials during Very Low Xenon Plasma Bombardment,” AIAA–2003–4561, 39th AIAA/ASME/SAE/ASEE Joint Propulsion Conference and Exhibit, Huntsville, AL, July 20–23, 2003.
54. Brophy, J.R., “Propellant Throughput Capability of the Dawn Ion Thrusters,” IEPC–2007–279, 30th International Electric Propulsion Conference, Florence, Italy, September 17–20, 2007.
55. Brophy, J.R., et al., “Development and Testing of the Dawn Ion Propulsion System,” AIAA–2006–4319, 42nd AIAA/ASME/SAE/ASEE Joint Propulsion Conference and Exhibit, Sacramento, CA, July 9–12, 2006.
56. Brophy, J.R., Polk, J.E., Randolph, T.M., and Dankanich, J.W., “Lifetime Qualification of Electric Thrusters for Deep-Space Missions,” AIAA–2008–5184, 44th AIAA/ASME/SAE/ASEE Joint Propulsion Conference & Exhibit, Hartford, CT, July 20–23, 2008.
57 Herman, D.A., Soulas, G.C., and Patterson, M.J., “NEXT Long-Duration Test after 11,570 h and 237 kg of Xenon Processed,” IEPC–2007–033, 30th International Electric Propulsion Conference, Florence, Italy, September 17–20, 2007.
58. Polk, J.E., Duchemin, O.B., Ho, C., and Koel, B.E., “The Effect of Carbon Deposition on Accelerator Grid Wear Rates in Ion Engine Ground Testing,” AIAA–2000–3662, 36th AIAA/ASME/SAE/ASEE Joint Propulsion Conference and Exhibit, Huntsville, AL, July 17–19, 2000.
59. Williams, G.J. and Gilland, J.H., “Modeling of the Accelerator Grid Erosion of the NASA Evolutionary Xenon Thruster (NEXT),” NEXT Internal Report, NASA Glenn Research Center, Cleveland, OH, September 2007.

REPORT DOCUMENTATION PAGE						*Form Approved* *OMB No. 0704-0188*

1. REPORT DATE *(DD-MM-YYYY)*
01-11-2010

2. REPORT TYPE
Technical Memorandum

3. DATES COVERED *(From - To)*

4. TITLE AND SUBTITLE
NASA's Evolutionary Xenon Thruster (NEXT) Project Qualification Propellant Throughput Milestone: Performance, Erosion, and Thruster Service Life Prediction After 450 kg

5a. CONTRACT NUMBER

5b. GRANT NUMBER

5c. PROGRAM ELEMENT NUMBER

6. AUTHOR(S)
Herman, Daniel, A.

5d. PROJECT NUMBER

5e. TASK NUMBER

5f. WORK UNIT NUMBER
WBS 346620.04.08.02.01.01

7. PERFORMING ORGANIZATION NAME(S) AND ADDRESS(ES)
National Aeronautics and Space Administration
John H. Glenn Research Center at Lewis Field
Cleveland, Ohio 44135-3191

8. PERFORMING ORGANIZATION REPORT NUMBER
E-17447

9. SPONSORING/MONITORING AGENCY NAME(S) AND ADDRESS(ES)
National Aeronautics and Space Administration
Washington, DC 20546-0001

10. SPONSORING/MONITOR'S ACRONYM(S)
NASA

11. SPONSORING/MONITORING REPORT NUMBER
NASA/TM-2010-216816

12. DISTRIBUTION/AVAILABILITY STATEMENT
Unclassified-Unlimited
Subject Category: 20
Available electronically at http://gltrs.grc.nasa.gov
This publication is available from the NASA Center for AeroSpace Information, 443-757-5802

13. SUPPLEMENTARY NOTES

14. ABSTRACT
The NASA's Evolutionary Xenon Thruster (NEXT) program is tasked with significantly improving and extending the capabilities of current state-of-the-art NSTAR thruster. The service life capability of the NEXT ion thruster is being assessed by thruster wear test and life-modeling of critical thruster components, such as the ion optics and cathodes. The NEXT Long-Duration Test (LDT) was initiated to validate and qualify the NEXT thruster propellant throughput capability. The NEXT thruster completed the primary goal of the LDT; namely to demonstrate the project qualification throughput of 450 kg by the end of calendar year 2009. The NEXT LDT has demonstrated 28,500 hr of operation and processed 466 kg of xenon throughput--more than double the throughput demonstrated by the NSTAR flight-spare. Thruster performance changes have been consistent with a priori predictions. Thruster erosion has been minimal and consistent with the thruster service life assessment, which predicts the first failure mode at greater than 750 kg throughput. The life-limiting failure mode for NEXT is predicted to be loss of structural integrity of the accelerator grid due to erosion by charge-exchange ions.

15. SUBJECT TERMS
Ion engines; Ion optics; Ion propulsion; Electric propulsion; Electrostatic propulsion; Plasma propulsion

16. SECURITY CLASSIFICATION OF:			17. LIMITATION OF ABSTRACT	18. NUMBER OF PAGES	19a. NAME OF RESPONSIBLE PERSON
					STI Help Desk (email:help@sti.nasa.gov)
a. REPORT	b. ABSTRACT	c. THIS PAGE			19b. TELEPHONE NUMBER *(include area code)*
U	U	U	UU	26	443-757-5802

Standard Form 298 (Rev. 8-98)
Prescribed by ANSI Std. Z39-18